Folding Topology of a Short Coiled-Coil Peptide Structure Templated by an Oligonucleotide Triplex

Lou, Chenguang; Christensen, Niels Johan; Martos-Maldonado, Manuel C; Midtgaard, Søren Roi; Ejlersen, Maria; Thulstrup, Peter W; Sørensen, Kasper K; Jensen, Knud J.; Wengel, Jesper

Published in:
Chemistry: A European Journal

DOI:
10.1002/chem.201700971

Publication date:
2017

Document version
Peer reviewed version

Citation for pulished version (APA):
Lou, C., Christensen, N. J., Martos-Maldonado, M. C., Midtgaard, S. R., Ejlersen, M., Thulstrup, P. W., ... Wengel, J. (2017). Folding Topology of a Short Coiled-Coil Peptide Structure Templated by an Oligonucleotide Triplex. Chemistry: A European Journal, 23(39), 9297–9305. DOI: 10.1002/chem.201700971

CHEMISTRY
A European Journal

A Journal of
ChemPubSoc Europe

Accepted Article

Title: Folding Topology of a Short Coiled Coil Peptide Structure Templated by an Oligonucleotide Triplex

Authors: Chenguang Lou, Niels Johan Christensen, Manuel C. Martos-Maldonado, Søren Roi Midtgaard, Maria Ejlersen, Peter W. Thulstrup, Kasper K. Sørensen, Knud J. Jensen, and Jesper Wengel

To be cited as: *Chem. Eur. J.* 10.1002/chem.201700971

Link to VoR: http://dx.doi.org/10.1002/chem.201700971

Supported by
ACES

WILEY-VCH

10.1002/chem.201700971

WILEY-VCH

Folding Topology of a Short Coiled Coil Peptide Structure Templated by an Oligonucleotide Triplex

Chenguang Lou,‡[a] Niels Johan Christensen,‡[b] Manuel C. Martos-Maldonado,[b] Søren Roi Midtgaard,[c] Maria Ejlersen,[a] Peter W. Thulstrup,[d] Kasper K. Sørensen,[b] Knud J. Jensen,*[b] and Jesper Wengel*[a]

Abstract: The rational design of a well-defined protein-like tertiary structure formed by small peptide building blocks is still a formidable challenge. Using peptide-oligonucleotide conjugates (POC) as building blocks, we here present the self-assembly of miniature coiled coil α-helical peptides guided by oligonucleotide duplex and triplex formation. POC synthesis was achieved by copper-free alkyne-azide cycloaddition between three oligonucleotides and a 23-mer peptide, which by itself exhibited multiple oligomeric states in solution. The oligonucleotide domain was designed to furnish a stable parallel triplex under physiological pH capable of templating the three peptide sequences to constitute a small coiled coil motif displaying remarkable α-helicity. The formed trimeric complex was characterized by ultraviolet thermal denaturation, gel electrophoresis, circular dichroism (CD) spectroscopy, small-angle X-ray scattering (SAXS), and molecular modeling. Stabilizing cooperativity was observed between the trimeric peptide and the oligonucleotide triplex domains, and an overall molecular size (~12 nm) was revealed in solution, independent of concentration. The topological folding of the peptide moiety differed strongly from those of the individual POC strands and the unconjugated peptide, exclusively adopting the designed triple helical structure.

Introduction

Nature has evolved complex biomolecules that play essential roles in organisms and that assemble into biomolecular nanostructures with remarkable precision.[1,2] Proteins constitute one family of large biomolecules with vast diversity and complexity.[3] They are composed of covalently linked amino acids to give primary sequences, which are further folded to form unique secondary, tertiary and quaternary structures through non-covalent interactions.[4] However, in living systems, usually only few of the many residues participate directly in enzyme catalysis and molecular recognition processes, and a limited number of the involved peptide strands partake in protein-protein recognition. In contrast, a relatively large portion of most proteins is responsible for conformational stability.[5-8] Inspired by Nature, *de novo* construction of functional man-made protein mimics from protein subunits and peptide sequences through non-covalent interactions is a research area of strong interest.[9-17]

Nucleic acids can form diverse secondary structures via intra- and intermolecular Watson-Crick base pairing and have been widely utilized to constitute elaborate nanostructures with high programmability and adaptability,[18-21] including protein assemblies.[13,22-34] Recently, we have demonstrated that self-assembly of three oligonucleotides (ONs), designed to form a triplex, each conjugated with a 30-mer peptide fragment known to form an inherently stable coiled coil structure, can lead to the formation in solution of a stable trimer with synergistic stabilization of both the ON triplex and the trimeric coiled coil moieties.[35] Herein, we advance this concept by studying the tendency of shorter peptides to form coiled coil structures templated by nucleic acid hybridization. In short, we demonstrate the assembly of a short (three heptad) coiled coil motif driven by ON hybridization to give a trimeric complex with a remarkable high degree of α-helicity (Figure 1). A combination of interstrand hydrophobic, electrostatic, and hydrogen bond interactions drive the formation of such α-helical coiled coils, one of the fundamental protein tertiary structures present in 5-10% of all known protein motifs.[36] With three heptad units along the sequence, two or more α-helical peptide strands wind around each other to generate right- or left-handed helical structures in various morphologies.[37] The length of the involved peptides influences the stability of the formed coiled coil structures. Herein, a 23-mer peptide sequence, derived from coil-V_aL_d[38] with an additional azidohexanoyl-Tyr residue at the N-terminal, was chosen as a model unit. In contrast to the full-length four-heptad coil-V_aL_d that has been reported to self-assemble into a stable trimeric coiled coil, this truncated version of coil-V_aL_d is not capable of forming a monodisperse trimeric coiled coil but appears as a mixture of monomeric, dimeric, and trimeric structures in solution.[39] Nucleic acid triple helical structures can be assembled with a triplex-forming oligonucleotide (TFO) binding within the major groove of a target duplex through Hoogsteen hydrogen-bonds.[40] Triple helices with a polypyrimidine-based TFO bound in a parallel orientation relative to the purine strand are usually more stable than

[a] C. Lou, M. Ejlersen, J. Wengel
Biomolecular Nanoscale Engineering Center, Department of Physics, Chemistry and Pharmacy
University of Southern Denmark
Campusvej 55, 5230 Odense M, Denmark
E-mail: jwe@sdu.dk
[b] N. J. Christensen, M. C. Martos-Maldonado, K.K. Sørensen, K. J. Jensen
Biomolecular Nanoscale Engineering Center, Department of Chemistry
University of Copenhagen
Thorvaldsensvej 40, 1871 Frederiksberg, Denmark
E-mail: kjj@chem.ku.dk
[c] S. R. Midtgaard
Niels Bohr Institute
University of Copenhagen
Universitetsparken 5, 2100 Copenhagen Ø, Denmark
[d] P. W. Thulstrup
Department of Chemistry
University of Copenhagen
Universitetsparken 5, 2100 Copenhagen Ø, Denmark

‡ C.L. and N.J.C. contributed equally to this work. Supporting information for this article is given via a link at the end of the document.

10.1002/chem.201700971

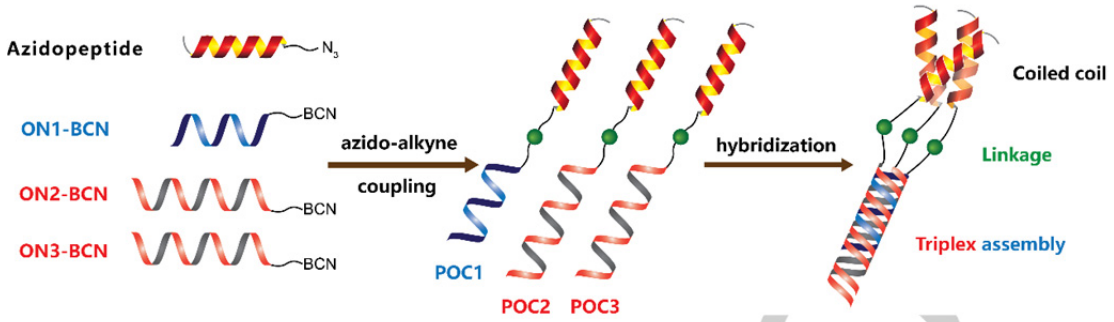

Figure 1. Self-assembly of a short coiled-coil motif by ON triplex formation involving three POCs formed via copper-free azide-alkyne coupling. BCN = bicyclo[6.1.0]nonyne.

antiparallel triple helices.[41] Favoring the former, we introduced 5-methyl-2'-deoxycytidine and locked nucleic acid (LNA) nucleotides into a TFO designed to furnish a parallel triple helix stable under physiological pH.[42,43] Conjugation of the 23-mer peptide to each strand of the oligonucleotide triple helix via copper-free azido-alkyne cycloaddition reactions yielded three peptide-oligonucleotide conjugates (POCs) which were used as building blocks for self-assembly of a short but stable trimeric coiled coil structure (Figure 1).

Results and Discussion

POC synthesis

Due to their high efficiency and functional group orthogonality, copper-free ring-strain promoted alkyne-azide cycloaddition reactions were employed to conjugate the 23-mer peptide to the three ONs (Figure 2a).[44] For ease of synthesis, the alkyne function was introduced on the 3'- or 5'-end of the ONs, while its azide reaction partner was introduced as azidohexanoyl-Tyr on the N-terminus of the peptide. Among commercially available strained cyclooctyne phosphoramidite monomers, bicyclo[6.1.0]nonyne (BCN) was chosen owing to its symmetric chemical structure and high reactivity (Figure 2b).[45] Further details on ON and peptide synthesis are included in the Supporting information. For the POC synthesis we have refined the method described in our previous work.[35] Therefore, with the desired ONs and peptide (**ON1-BCN**, **ON2-BCN** or **ON3-BCN,** and **azidopeptide**, Figure 2b and Figure S2) at hand, the copper-free azide-alkyne coupling reactions were carried out under microwave heating at micromolar concentrations using one equivalent of BCN-bearing ON and 1.25 equivalent **azidopeptide** in a solvent system of DMSO and Milli-Q water (1:1, v/v). As expected, crude **POC1** was water-soluble. Interestingly, unlike the corresponding crude POCs containing the 30-mer peptide[35] (insoluble in Milli-Q water), **POC2** and the majority of **POC3** (~80%) were easily dissolved in Milli-Q water, though a minor portion of **POC3** (~20%) still required assisted solvation from a buffer solution (0.025 M Tris-HCl, 0.01 M sodium perchlorate, pH 7.6). The remaining azidopeptide was removed upon repeated precipitation from acetonitrile/ethanol (1:1, v/v). The separation of POCs from their corresponding ON-BCN building blocks was challenging on ion-exchange HPLC, but reversed-phase HPLC purification afforded the three desired POCs in overall yields of ~70% taking advantage of the higher lipophilicity of the POCs relative to that of the unconjugated ONs In this way, an efficient and high-yielding synthesis protocol was established for water-soluble POCs using only 1.25 equivalents of azido-functionalized peptide relative to BCN-labelled ONs (further details are included in the Experimental section and in Figure S3 and Figure S4).

Ultraviolet thermal denaturation and gel electrophoresis studies

With **POC1**, **POC2**, **POC3** and their corresponding ON controls (**ON1**-**ON3**) in hand, the thermal stability of duplex and triplex domains was evaluated to validate the fidelity of Watson-Crick and Hoogsteen recognition for 12 different assemblies with varying numbers of peptide strands attached (Table 1). Whereas a cooperative stabilizing effect was noticed when we employed the 30-mer four-heptad peptide strands due to the inherent stability of the corresponding three-stranded coiled coil structures,[35] the 23-mer peptide used herein is too short to assemble into stable, monodisperse two- or three-stranded helical coiled coil structures by itself.[39] Therefore, one aim was to investigate whether the confinement of two or three of such shorter peptide strands to the terminals of hybridized ON domains would lead to a stabilizing effect on duplex and triple helical assemblies. For duplex denaturation studies, the wavelength 260 nm of maximum ultraviolet absorbance was used (Figure S5) whereas for triplex denaturation studies 275 nm was chosen, which is near the maximal ultraviolet absorbance difference between the triple helix and the underlying duplex while still being separated from the duplex maximum absorbance wavelength (Figure S5). Relative to ONs, the ultraviolet absorption of the peptide units and coiled coil structures were considered negligible at these two wavelengths (Figure S5 and Figure S6).

In the case of duplex systems, the attached peptide strands had no significant influence on the thermal stability, regardless if one or two peptide strands were anchored (Table 1, entry 1-4). This is in stark contrast to the significant duplex stabilizing effect observed earlier by the conjugation of two 30-mer peptide strands.[35] We ascribe the loss of stabilizing cooperativity to

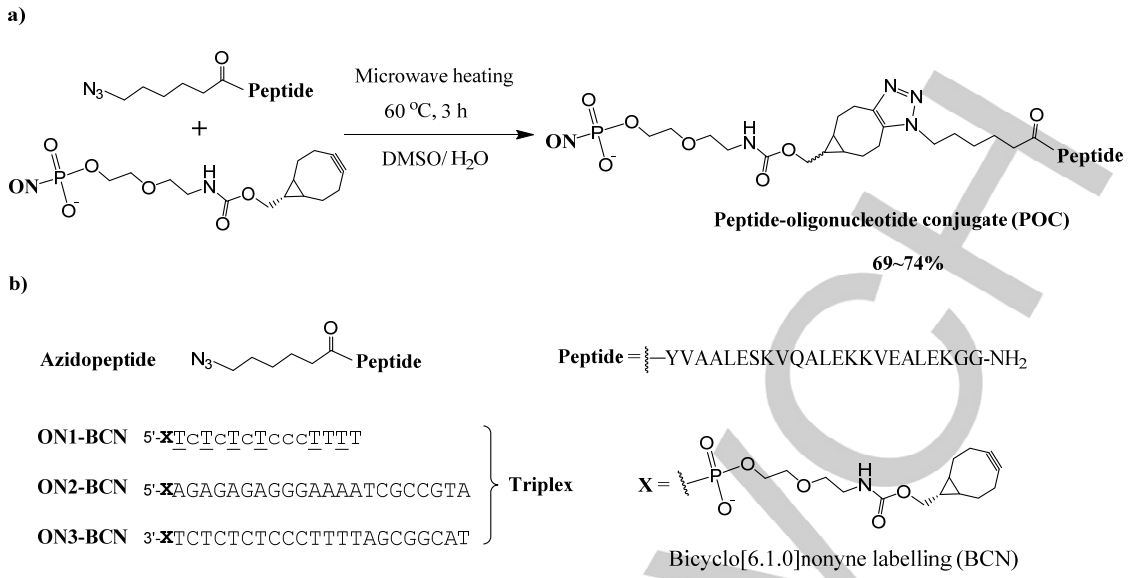

Figure 2. Synthesis of three peptide-ON conjugates (POCs). A) The click reactions occurred between azidopeptide and BCN-functionalized ONs. B) Sequences of **azidopeptide** and **ON1-BCN**, **ON2-BCN** and **ON3-BCN**, T = LNA-T monomer; c = 5-methyl-2'-deoxycytidine monomer; A, G, C and T = DNA monomers.

the reduced intermolecular affinity between the truncated peptide sequences. This indicates that the length of the peptide segment can be used to control the dynamics of these protein mimics. All four duplex systems studied gave almost identical melting (T_m) and annealing (T_a) temperature values, and furthermore almost superimposable dissociation and association curves (Figure S7). This demonstrates thermal reversibility of Watson-Crick interactions for all duplexes, and furthermore highlights the dominance of the nucleic acid fragment with respect to formation of the bimolecular assemblies.

ON1 or **POC1** was used as TFO to bind to the major groove of the above mentioned four duplexes in construction of eight parallel triplexes. In comparison with **ON1**+**ON2**+**ON3** (Table 1, entry 5), substantial increase in triplex melting temperature was exclusively observed when the peptide unit was simultaneously present on all three ON strands (Table 1, entry 6), clearly reflecting formation of a three-stranded coiled coil peptide structure and a cooperative stabilization between this trimeric peptide bundle and the ON triplex domain. This supports that the stable tertiary structure of the peptide domain is promoted by the hybridization of the ON-parts of the three POC units employed. Notably, the non-conjugated peptide[39] was incapable of forming a stable coiled coil structure under similar conditions. This cooperativity, *i.e.* synergistic stabilization between the ON and peptide structural elements, was further substantiated by the fact that **POC1**+**POC2**+**POC3** produced a clear triplex annealing transition not observed for the **ON1**+**ON2**+**ON3** triple helix (Table 1, entry 6). There was no significant stabilizing effect observed for any of the other six triplex structures containing only one or two peptide strands (Table 1, entry 7-12; Figure S8), accentuating that all parts of the triple-stranded peptide bundle are necessary for formation of a stable coiled coil structure. Intriguingly, reassembly of the ON triplex was still accelerated during the annealing process with only two peptide units being present, one on the TFO strand and the other on either strand of the underlying duplex. Both **POC1**+**POC2**+**ON3** and **POC1**+**ON2**+**POC3** thus exhibited clear annealing transitions, though their triplex annealing temperatures were lower than the one observed for the **POC1**+**POC2**+**POC3** complex (Table 1, entry 10 and 11; Figure S8). Compared to **POC1**+**POC2**+**POC3** where the triplex annealing profile nicely matched the corresponding melting transition, the kinetically slower triplex reassembly for **POC1**+**POC2**+**ON3** and **POC1**+**ON2**+**POC3** is explained by the absence of the third peptide unit leading to less synergy during the assembly process. It is noteworthy that there were no obvious changes in melting and annealing temperature for the underlying duplexes, which indicates that the binding of **ON1** or **POC1** did not significantly perturb the duplex stability as also reported earlier for the corresponding duplexes containing the 30-mer peptide strand.[35]

The thermal stability of the parallel ON triplex is dependent on both pH and ionic strength.[46,47] An increase in pH would lead to the deprotonation at N3 of cytosine nucleobases in the TFO and subsequent destabilization of the C^+•GC triplet, and a decrease in ionic strength would lead to increased electrostatic repulsion between three negatively charged phosphate backbones and a destabilized triplex. An experiment was performed with the fully conjugated **POC1**+**POC2**+**POC3** complex and the **ON1**+**ON2**+**ON3** triple helix control at pH 8 under two different ionic strengths (5.8 mM phosphate buffer containing 100 mM NaCl and 0.1 mM EDTA or 6.7 mM phosphate buffer containing 0.1 mM EDTA but without NaCl) (Figure S9). As expected the increase in pH severely destabilized the **ON1**+**ON2**+**ON3** triplex, but both triplex melting and annealing transitions were clearly noticed for **POC1**+**POC2**+**POC3** (pH 8; 5.8 mM phosphate buffer containing 100 mM NaCl and 0.1 mM EDTA). Further decrease in

10.1002/chem.201700971

Table 1. UV-melting studies*

A

ON1	5'-TcTcTcTcccTTTT
ON2	5'-AGAGAGAGGGAAAATCGCCGTA
ON3	5'-TACGGCGATTTTCCCTCTCTCT
POC1	5'-QTcTcTcTcccTTTT
POC2	5'-QAGAGAGAGGGAAAATCGCCGTA
POC3	5'-TACGGCGATTTTCCCTCTCTCTQ

Q = 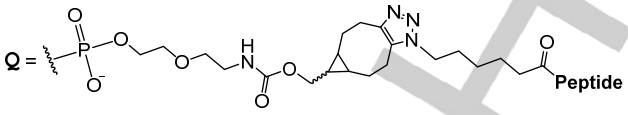

Peptide = —YVAALESKVQALEKKVEALEKGG-NH_2

B

Entry	Duplex/Triplex	Melting	Annealing	Structure
1	**ON2+ON3**	65.2 ± 0.2 °C	65.3 ± 0.2 °C	
2	**POC2+ON3**	65.1 ± 0.2 °C	65.4 ± 0.2 °C	
3	**ON2+POC3**	65.1 ± 0.3 °C	65.3 ± 0.2 °C	
4	**POC2+POC3**	65.4 ± 0.1 °C	65.6 ± 0.2 °C	
5	**ON1+ON2+ON3**	39.6 ± 0.3 °C (65.9 ± 0.4 °C)	n.d. (65.8 ± 0.2 °C)	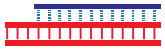
6	**POC1+POC2+POC3**	50.3 ± 0.2 °C (66.5 ± 0.1 °C)	50.4 ± 0.1 °C (66.3 ± 0.2 °C)	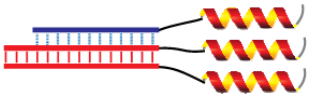
7	**ON1+POC2+ON3**	40.9 ± 0.1 °C (65.3 ± 0.2 °C)	n.d. (65.4 ± 0.2 °C)	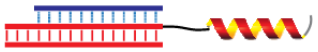
8	**ON1+ON2+POC3**	40.8 ± 0.1 °C (66.2 ± 0.3 °C)	n.d. (66.3 ± 0.2 °C)	
9	**ON1+POC2+POC3**	40.9 ± 0.2 °C (66.4 ± 0.3 °C)	n.d. (66.5 ± 0.3 °C)	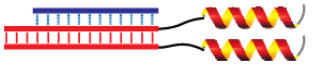
10	**POC1+POC2+ON3**	41.2 ± 0.2 °C (64.8 ± 0.2 °C)	30.9 ± 0.6 °C (65.2 ± 0.1 °C)	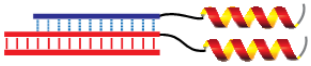
11	**POC1+ON2+POC3**	41.1 ± 0.4 °C (65.0 ± 0.3 °C)	35.3 ± 0.4 °C (65.1 ± 0.1 °C)	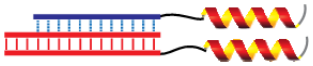
12	**POC1+ON2+ON3**	40.4 ± 0.1 °C (65.5 ± 0.1 °C)	n.d. (65.5 ± 0.2 °C)	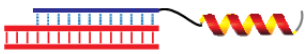

*[a] POC and ON sequences: T = thymine LNA monomer; c = 5-methyl-2'-deoxycytidine DNA monomer; A, C, G and T are DNA monomers. [b] Thermal denaturation and annealing temperatures (T_m and T_a values) of POC-including and ON-reference duplexes (entries 1-4) and triple helixes (entries 5-12) at pH 7.0 measured as an average of three independent melting temperature determinations shown with the corresponding standard deviations. For entries 5-12, the values in brackets are T_m and T_a values measured for the corresponding underlying duplexes. n.d. = not detected. The experiments were recorded at 260 nm or 275 nm in 5.8 mM NaH_2PO_4/Na_2HPO_4 buffer (pH 7.0) containing 100 mM NaCl and 0.10 mM EDTA. The concentration of the individual duplex components was 1.0 μM, while the TFO component was used in 1.5 μM concentration. The peptide moiety is marked alternating yellow and red, the TFO moiety in blue, and the DNA duplex moiety in red.

ionic strength (6.7 mM phosphate buffer containing 0.1 mM EDTA but without NaCl) abolished the triplex annealing transition, though the melting transition was preserved. Again, we attribute this extraordinary stability to the cooperativity between the ON triplex and the peptide bundle. In comparison, only a very weak triplex melting transition was detected for

ON1+**ON2**+**ON3** at pH 8 (5.8 mM phosphate buffer containing 100 mM NaCl and 0.1 mM EDTA). Notably, these results are consistent with gel electrophoresis and circular dichroism experiments (*vide infra*).

Duplex and triplex assembly was also characterized using non-denaturing polyacrylamide gel electrophoresis (native-PAGE) for **ON2+ON3**, **POC2+POC3**, **ON1**+**ON2**+**ON3** and **POC1**+**POC2**+**POC3** (Figure 3) carried out at low temperature and relatively low voltage to minimize possible dissociations of the triple helical structures. As expected, the ON duplex control **ON2**+**ON3** (Figure 3, lane 1) was located close to the 20-mer DNA marker. When both strands were conjugated to the peptide, significant mobility retardation was noticed (**POC2+POC3**; Figure 3, lane 2), which is attributed to the higher mass-to-charge ratio and increased molecular size. The binding of **ON1** to the major groove of **ON2**+**ON3** slightly reduced the on-gel mobility, showing **ON1**+**ON2**+**ON3** (Figure 3, lane 3) as a major band with an electrophoretic mobility close to that of the 25-mer DNA marker. The smearing region in front may be caused by minor dissociation of **ON1** from the triple helix. With **POC1**+**POC2**+**POC3** (Figure 3, lane 4) a single and clean band was observed displaying the least mobility among the complexes studied. In a concentration array, **POC1**+**POC2**+**POC3** uniformly appeared as one single band (even up to 25 μM, 1:1:1 stoichiometric ratio), signifying a monodisperse assembled trimeric complex in solution in all concentrations tested (Figure S10). This behavior is in sharp contrast to our previous work where the attachment of the 30-mer peptide to the corresponding duplexes and triplexes induced dimerization or aggregation, in a concentration dependent manner.[35]

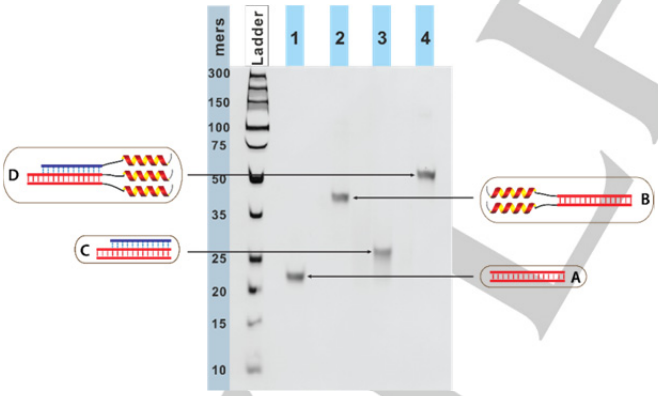

Figure 3. Gel electrophoresis. Non-denaturing 13% PAGE at pH 7.0 and 4 °C: lane 1, **ON2**+**ON3** (structure shown as 'A'); lane 2, **POC2**+**POC3** (structure shown as 'B'); lane 3, **ON1**+**ON2**+**ON3** (structure shown as 'C'); lane 4, **POC1**+**POC2**+**POC3** (structure shown as 'D'). The gel was visualized by ultraviolet excitation at 260 nm after ethidium bromide staining. The O'GeneRuler Ultra Low Range DNA Ladder from bottom to top: 10, 15, 20, 25, 35, 50 75, 100, 150, 200 and 300 mers. The peptide moiety is marked alternating yellow and red, the TFO moiety in blue, and the DNA duplex moiety in red.

This implies that the propensity of oligomerization for such nanoscale assemblies can be modulated by fine-tuning structure and composition of the peptide motif. Unsurprisingly, an increase to pH 8 led to a full decomposition of **POC1**+**POC2**+**POC3** on the gel, which is ascribed to the lower triplex stability and a higher propensity of **POC1** of being dissociated from the triple helical structure during the electrophoresis (Figure S11).

Circular dichroism spectroscopy

As can be seen from Figure 4, **POC1+POC2+POC3** exhibited a very intense α-helical signal at a total peptide concentration of 9 μM. In contrast, this intense α-helical signal was not observed for the **azidopeptide** and the individual POCs at the same concentration. This is clear evidence of the efficiency of the triplex ON scaffold for the assembly of the coiled coil motif. The magnitude of the α-helical signal of **POC1+POC2+POC3** was extraordinarily high. The mean residue ellipticity values were similar to those reported for the triplex POC assembly containing the 30-mer peptide strands which as unconjugated peptides are much more prone to coiled coil formation.[35] To the best of our knowledge, there are no precedents of such high α-helical value in purely aqueous solvents at room temperature, but Walliman *et al* have reported similar observations for an N-terminally templated lysine-rich peptide in an ethylene glycol-water mixture at pH 1 and below 0 °C.[48] Remarkably, in our case the **azidopeptide** did not reach similar mean residue ellipticity values, even at 220 μM (Figure S12).

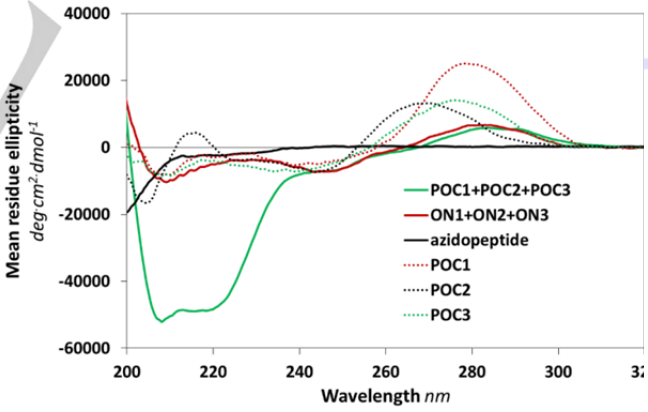

Figure 4. CD spectra (mean residue ellipticity) of **POC1+POC2+POC3** (3:3:3 μM, green), **ON1+ON2+ON3*** (3:3:3 μM, red), **azidopeptide** (9 μM, black), **POC1** (9 μM, red dotted line), **POC2** (9 μM, black dotted line) and **POC3** (9 μM, green dotted line) at 20 °C in 5.8 mM sodium phosphate buffer at pH 7.0 with 100 mM NaCl and 0.1 mM EDTA. The corresponding references (buffer solutions) were subtracted from each spectrum. *Mean residue ellipticity for **ON1**+**ON2**+**ON3** was calculated as for **POC1**+**POC2**+**POC3**, individual POCs and **azidopeptide**; molar ellipticity (calculated for a total concentration of 9 μM) was divided by 23 (the number of peptide residues in **azidopeptide**/POCs).

The triplex **ON1+ON2+ON3** was measured to evaluate the contribution of the ON part of **POC1+POC2+POC3** to the ellipticity in the alpha helix region. The signals at 208 and 222 nm (where the two characteristic α-helix minima are observed) were 9.8% and 18.4% of that of **POC1+POC2+POC3**, respectively. In contrast, the same peptide moiety has been covalently attached to carbohydrate scaffolds via its C-terminal to give rise to the so-called carboproteins, each molecule comprising a carbohydrate template and three peptides where the carbohydrate scaffold induced coiled coil formation.[49] However, even at a much higher peptide concentration (150 μM), the reported magnitude of the α-helicity for those carboproteins was still significantly lower than that for **POC1+POC2+POC3** (3:3:3 μM).

It was also interesting that at the same total peptide concentration, duplex **POC2+POC3** (4.5:4.5 μM) showed a conspicuous α-helical signal (Figure S13). This reflects that the ON duplex scaffold may preserve the templating ability to promote a double-helical coiled coil formation thus providing the high degree of α-helicity, despite a reduced intensity compared to the corresponding **POC1+POC2+POC3**. The T_m value for the peptide unfolding of **POC1+POC2+POC3** was estimated to ~54 °C from a temperature series at 220 nm (Figure S14), which was also notable since the non-conjugated **azidopeptide** did not show any secondary structure even at 20 °C at the same concentration. Compared to the T_m value of 50.3 °C obtained from ultraviolet melting measurements (Table 1 and Figure S8), the peptide transition obtained by CD gave a slightly higher T_m value, possibly indicating that the dissociation of TFO started from 3'-end due to the cooperative stabilization between the ON triplex and coiled coil domains.

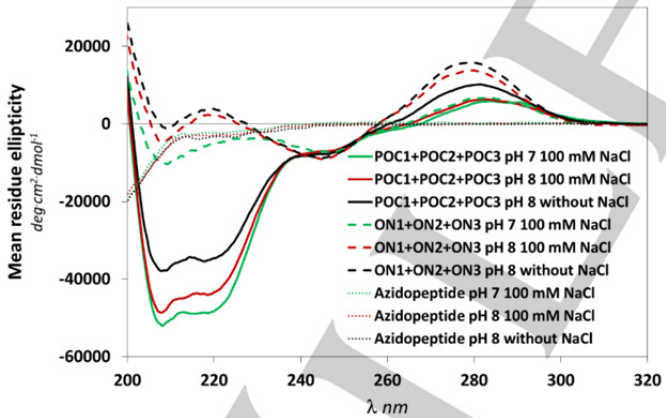

Figure 5. CD spectra (Mean residue ellipticity) of **POC1+POC2+POC3** (3:3:3 μM, —), **ON1+ON2+ON3*** (3:3:3 μM, - - -) and **azidopeptide** (9 μM, ···), at 20 °C in three different buffers; 5.8 mM sodium phosphate buffer at pH 7.0 with 100 mM NaCl and 0.1 mM EDTA (green), 5.8 mM sodium phosphate at pH 8.0 with 100 mM NaCl and 0.1 mM EDTA (red) and 6.7 mM sodium phosphate at pH 8.0 containing 0.1 mM EDTA but without NaCl (black). The corresponding references (buffer solutions) were subtracted from each spectrum. *Mean residue ellipticity for **ON1**+**ON2**+**ON3** was calculated as for **POC1**+**POC2**+**POC3** and **azidopeptide**; molar ellipticity (calculated for a total concentration of 9 μM) was divided by 23 (the number of peptide residues in **azidopeptide**/POCs).

The CD spectra of **azidopeptide**, **POC1+POC2+POC3** and **ON1+ON2+ON3** were measured at pH 8.0 under two different ionic strengths (Figure 5). As mentioned previously, the increase in pH and a decrease in ionic strength destabilize the ON triplex. When the pH was increased to 8, the maximum for **ON1+ON2+ON3** in the near ultraviolet region was hypsochromically shifted with a concomitant intensity increase. We ascribe these changes to the transition from triplex to duplex. The decrease in the ionic strength led to further changes with the same tendency, although to a lesser extent. In contrast, for **POC1+POC2+POC3** the pH increase induced limited changes at higher wavelengths, and only a small decrease in the intensity of the α-helix signal. This indicated that the triplex motif to a large extent was preserved, thus highlighting the stabilizing synergy between the peptide and ON motifs in the tri-molecular assembly. When the ionic strength was simultaneously reduced, a clear hypsochromic shift and an increase of the intensity of the maximum at higher wavelength was observed, together with a more significant decrease of the intensity of the α-helical signal. Nonetheless, the magnitude of the variation at higher wavelength was lower than that observed for **ON1+ON2+ON3** when only the pH was increased. This pointed to only partial dissociation of the triplex forming strand even under such harsh condition at 20 °C, which was consistent with the T_m value (26.4 °C) of **POC1+POC2+POC3** measured in low salt buffer (pH 8.0, 6.7 mM sodium phosphate with 0.1 mM EDTA).

The $\theta_{222}/\theta_{208}$ ratio can be calculated from the CD spectroscopic data. This ratio reflects the degree of helix association, such that values above unity reflect coiled-coil formation, whereas values ≤ 0.86 are observed for isolated helices.[50,51] The obtained $\theta_{222}/\theta_{208}$ ratio is concentration dependent in the current case, where oligomerization is required to form a coiled-coil structure. For the sample containing **POC1**, **POC2**, **POC3** at a concentration of 3 μM each, the $\theta_{222}/\theta_{208}$ ratio is close to unity (0.99) after subtracting the CD contributions from the corresponding oligonucleotide triplex (**ON1**, **ON2**, and **ON3** at a concentration of 3 μM each). At a 9 μM concentration the **azidopeptide** did not have any significant α-helical CD signal, thus the ratio was not calculated. In our recent study on a POC with a four-heptad repeat in the peptide, $\theta_{222}/\theta_{208}$ ratios equal to 1.03 and 1.05 were observed for the four-heptad **azidopeptide** alone and for the POC triplex, respectively.[35] Also, in a study of the unconjugated four-heptad repeat peptide, a $\theta_{222}/\theta_{208}$ ratio of 1.02 was reported (the CoilVaLd-YG peptide), while related three-heptad repeat peptides gave much lower ratios.[39] In both the POC and peptide cases the reported $\theta_{222}/\theta_{208}$ ratios were determined for higher concentrations of peptide/POCs than in the present study.

SAXS and molecular modelling of the POC solution structure.

Small-angle X-ray scattering (SAXS) was performed to investigate the structure of **POC1**+**POC2**+**POC3** in solution, both in regard to oligomeric state and overall structure. Two concentrations, 10 μM and 50 μM were measured (Figure S15 - 17) as our previous study on a POC containing a 30-mer peptide

indicated concentration-dependent oligomerization.[35] It is evident from the total scattering that a trimeric assembly is formed at both concentrations, indicating concentration-independent self-assembly of **POC1**+**POC2**+**POC3** above a certain threshold. This suggests that the oligomeric state of assembled protein mimics could be fine-tuned by the peptide length. From overlaying the two datasets and the indirect Fourier transformations (Figure S16 and S17) it is clear that the data, and hence the structures, are identical and have an overall length of around 11 nm. Key parameters are summarized in Table 2.

To allow a detailed structural interpretation of the SAXS data, we constructed a molecular model of the POC trimer (Figure S18-21), see Methods Section for details. The calculated scattering from the final molecular model fits against SAXS measurements both at 50 μM (shown in Figure 6) and 10 μM (shown in Figure S21). The molecular model reproduces the overall shape of the SAXS measurements at both concentrations. Taken together with the similarity of experimental SAXS data at 50 μM and 10 μM (Figure S16 and 17), this supports that the POC system maintains the same oligomerization state at both concentrations.

Table 2 SAXS parameters for the POC1+POC2+POC3 system at 10 μM and 50 μM.

Conc. (μM)	D_{max} (Å)	Oligomeric state	R_g (Å)	$I(0)_{exp}$ (cm^{-1})	$I(0)_{calc}$ (cm^{-1})
10	109.93±4.87	trimer	31.16±0.20	0.0126	0.01439
50	117.08±1.69	trimer	33.15±0.11	0.0774	0.07197

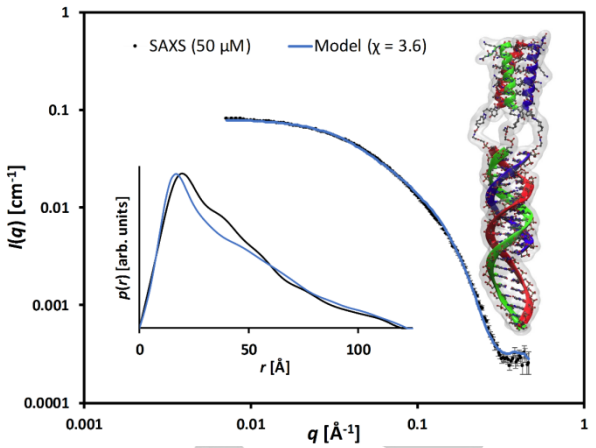

Figure 6. Comparison of measured and predicted SAXS data for **POC1+POC2+POC3.** Measurements (50 μM POC concentration) are shown in black. Predictions are shown in blue. Main figure: Measured scattering curve with grey errorbars against model fit. χ is the FoXS goodness-of-fit parameter. Left inset: Pair distance distribution functions ($p(r)$) for measured and predicted SAXS. Right inset: Molecular model used for SAXS predictions.

A close inspection of the 50 μM data (Figure 6 and Figure S20) can be justified due to the better signal-to-noise ratio compared to the 10 μM measurements. The semi-log SAXS plot (Figure S20) shows a strong agreement between prediction and measurement for $0 \le q \le 0.2$ Å^{-1}. The model underestimates the measurements somewhat for $0.2 \le q \le 0.3$ Å^{-1}. For $q \ge 0.3$ Å^{-1}, several factors may account for the discrepancy between model and measurement, including inherent difficulties in modelling the solvation layer and subtle structural variations and dynamics. The larger experimental errors in this region likely reflect the dynamic nature of the fine-structure of the POC in solution. These uncertainties are more pronounced at the low (10 μM) POC concentration (Figure S21). Despite these discrepancies, the overall good agreement between predicted and measured SAXS data supports that a single trimeric POC species is present in both 10 μM and 50 μM solutions with a similar extended conformation. The molecular model shown in Figure 6 (right inset) is our best prediction of this solution structure.

Conclusions

We designed peptide-oligonucleotide constructs to assemble into a very short hetero-trimeric coiled coil motif by nucleic acid hybridization. A convenient and highly efficient method was developed for synthesis of water-soluble peptide-oligonucleotide conjugates via copper-free azide-alkyne cycloaddition reactions using only 1.25 equivalents of azidopeptide relative to the appropriate BCN-labelled oligonucleotides. Self-assembly of the three conjugates gave the desired trimeric complex. Ultraviolet thermal denaturing studies showed that the simultaneous presence of three peptides cooperatively stabilized the oligonucleotide triplex domain and that the peptide attachment was fully compatible with Watson-Crick and Hoogsteen base-pairing. Native non-denaturing gel electrophoresis provided further evidence for the formation of the designed trimeric assembly. CD spectroscopy demonstrated an extraordinarily high degree of α-helicity for the peptide domain of the complex. SAXS structural analysis showed that the assembly of the three oligonucleotide-peptide conjugates leads to the formation of a trimeric complex at the concentrations (10 μM and 50 μM) studied. Molecular modelling constrained by SAXS measurements suggested a single trimeric complex with an extended conformation. In conclusion, these results validate the potential of building artificial protein mimics from peptide sequences using the driving force of nucleic acid hybridization. The results also underline the relevance of peptide structure, as herein shown for peptide length, as a determining factor for stability and composition of designer nanostructures.

Experimental Section

Synthesis of POC1, POC2 and POC3 (see Figure S3 for further details). **ON1-BCN** (89 nmol, 0.49 mL, dissolved in Milli-Q water) was added to a solution of **azidopeptide** (112 nmol) in DMSO (1.00 mL) before H_2O (0.51 mL) was added. The resulting solution was transferred to a Biotage microwave reaction vial (2 mL) and sealed under an atmosphere of nitrogen. The reaction was carried out on a Biotage Initiator microwave synthesizer at 60 °C for 3 h whereupon all solvents were removed *in vacuo* and the residue was re-dissolved in Milli-Q water. The same

synthesis procedure was repeated two times. The three crude solutions (from 267 nmol **ON1-BCN**) were combined and evaporated *in vacuo*. The residue was precipitated to remove excess peptide by first adding two aqueous solutions of sodium acetate (3 M, 15 µL) and sodium perchlorate (5 M, 15 µL) followed by addition of a cold solvent system of acetonitrile and ethanol (1.5 mL, 1:1, v/v; -20 °C). The resulting suspensions were stored at -20 °C for 1 h, and after centrifugation (13200 rpm, 5 min, 4 °C) the supernatants were removed and the pellet further washed with cold solvents (2 × 1 mL; ethanol/acetonitrile, 1:1 - 20 °C), dried for 30 min under a flow of nitrogen. The precipitation and washing process was repeated one more time before the pellet was re-dissolved in triethylammonium acetate buffer (0.05 M,1 mL) for further purification.

The same preparation protocol was applied on synthesis of **POC2 and POC3** (Fig. S3): **ON2-BCN** (142 nmol, 0.98 mL, dissolved in Milli-Q water) was added into a solution of **azidopeptide** (178 nmol) in DMSO (0.98 mL). After 3 h microwave-assisted reaction, the solvents were evaporated *in vacuo*, and the residue was precipitated in a solvent system of acetonitrile and ethanol (1:1, v/v) for two times as aforementioned. The pellet was then dissolved in triethylammonium acetate buffer (0.05 M, 1 mL) for further purification. **ON3-BCN** (100 nmol, 0.95 mL, dissolved in Milli-Q water) was added into a solution of **azidopeptide** (125 nmol) in DMSO (1.05 mL). After the solvents were removed *in vacuo*, the residue was subsequently rinsed with Milli-Q water and buffer (0.025 M Tris-HCl, 0.01 M sodium perchlorate, pH 7.6) to obtain ~80% and ~20% crude POCs in water and buffer phase, respectively. The synthesis procedure was repeated two times. Both crude water phase and buffer phase solutions (300 nmol) were combined individually and evaporated *in vacuo* to remove the solvents. Each residue was precipitated twice in a solvent system of acetonitrile and ethanol (1:1, v/v) in the same way. The two pellets were then separately dissolved in triethylammonium acetate buffer (0.05 M, 1 mL×2) for further purification.

Purification and analysis. The four crude POCs (**POC1**, **POC2**, **POC3** water phase and **POC3** buffer phase) were purified by RP-HPLC using a Waters System 600 HPLC equipment equipped with a Waters XBridge BEH C18-column (5 µm, 100 mm × 19 mm). Elution was performed starting with an isocratic hold of A-buffer for 2 min followed by a linear gradient to 70% B-buffer over 16.5 min at a flow rate of 5.0 mL/min (A-buffer: 0.05 M triethylammonium acetate in Milli-Q water, pH 7.4; B-buffer: 25% A-buffer, 75% acetonitrile). After removal of the solvents under a flow of nitrogen, the resulting solutions were desalted via precipitation by first adding two aqueous solutions of sodium acetate (3 M, 15 µL) and sodium perchlorate (5 M, 15 µL) followed by addition of cold ethanol (1 mL, 99% w/w; -20 °C). The resulting suspensions were stored at -20 °C for 1 h, and after centrifugation (13200 rpm, 5 min, 4 °C) the supernatants were removed and the pellet further washed with cold ethanol (2 × 1 mL; -20 °C), and dried for 30 min under a flow of nitrogen. The precipitation and washing process was repeated one more time. The pellet was then dissolved in Milli-Q water (1.0 mL) to give **POC1** (188 nmol, 70%)**, POC2** (105 nmol, 74%) and **POC3** (206 nmol, 69%, 157 nmol from water phase and 49 nmol from buffer phase), respectively. Mass spectra of POCs were recorded on a Bruker Daltonics Microflex LT MALDI-TOF MS instrument in ES^+ mode (representative MS in Fig. S4). Analytical IE-HPLC traces were recorded on a Merck-Hitachi Lachrom system equipped with a DNAPac PA100 analytical column (13 µm, 250 mm × 4 mm) heated to 60 °C. Elution was performed with an isocratic hold of buffer B (10 %), starting from 2 min hold on 2 % Buffer A in Milli-Q water, followed by a linear gradient to 30% buffer A in 23 min at a flow rate of 1.1 mL/min (buffer A: 1.0 M sodium perchlorate; buffer B: 0.25 M Tris-Cl, pH 8.0) (representative IE-HPLC traces in Figure S4). Concentrations of purified POCs were determined by UV at 260 nm.

CD spectroscopy. Far UV CD data were recorded on a JASCO J-815 calibrated with ammonium d-10-camphorsulfonate and the data acquired using 0.1 or 0.2 cm path-length cells from Hellma. CD temperature series were performed between 20 and 90 °C in a thermostated cell holder in the CD instrument. Temperature series were measured at + 1 °C intervals. T_m values was determined as maximum of the first derivative of the temperature series.

Molecular Modelling. We constructed an initial molecular model of the POC triplex by first building the oligonucleotide structure (**ON1**+**ON2**+**ON3**) in BIOVIA Discovery studio visualizer[52] as all-triplex with an arbitrary extra oligonucleotide strand on **ON1** to give it the same length as **ON2** and **ON3**. Subsequently, we removed the extra nucleotides on **ON1** to yield the duplex/triplex topology of the (**ON1**+**ON2**+**ON3**) structure. The linkers (Q in Table 1A) were constructed in Maestro, and subjected to a short conformational search in Macromodel,[53] from which extended conformations were selected. The ON triplex and extended linkers were combined and attached via the linkers to the short peptide generated by editing the coil-V_aL_d crystal structure[38] in Maestro. The resulting POC trimer model was solvated in an orthorhombic box of 63449 TIP3P water molecules[54] with charge neutralizing Na^+ counterions and an additional 0.15 M NaCl ionic background. The solvated system was subjected to 10 ns molecular dynamics simulation in the NPT ensemble (standard pressure and temperature) in Desmond[55] using the OPLS_2005 force field[56] with positional harmonic restraints on the oligonucleotide atoms. 1000 structural snapshots were extracted from the MD trajectory with VMD[57] and used as input to FOXS[58,59] to predict SAXS scattering curves from the different conformations of the molecular model (excluding hydrogens) and to carry out fitting against experimental SAXS data obtained at 10 µM and 50 µM, respectively. Extended conformations from the first ~1 ns of the MD trajectory generally provided better fits against experimental data than less linear conformations sampled from the last half of the simulation (Figure S18). The MD structure minimizing the FoXS goodness of fit measure χ was selected and refined further (Supporting Information S9), yielding the final approximation of the POC structure in solution.

Acknowledgements

The VILLUM FONDEN is thanked for funding Biomolecular Nanoscale Engineering Center (BioNEC), a VILLUM center of excellence, grant number VKR022710. Joan Hansen and Tina Grubbe Hansen are thanked for technical assistance on oligonucleotide synthesis and purification.

Keywords: oligonucleotides • peptides • click chemistry • molecular modeling • cicular dichroism

[1] J. A. Marsh, H. Hernandez, Z. Hall, S. E. Ahnert, T. Perica, C. V. Robinson, S. A. Teichmann, *Cell* **2013**, *153*, 461-470.
[2] P. Tompa, *Chem. Soc. Rev.* **2016**, *45*, 4252-4284.
[3] B. J. G. E. Pieters, M. B. van Eldijk, R. J. M. Nolte, J. Mecinovic, *Chem. Soc. Rev.* **2016**, *45*, 24-39.
[4] J. A. Marsh, S. A. Teichmann, *Annu. Rev. Biochem.*. **2015**, *84*, 551-575.
[5] M. W. Peczuh, A. D. Hamilton, *Chem. Rev.* **2000**, *100*, 2479-2493.
[6] A. Ramanathan, A. Savol, V. Burger, C. S. Chennubhotla, P. K. Agarwal, *Acc. Chem. Res.* **2014**, *47*, 149-156.
[7] J. Gavenonis, B. A. Sheneman, T. R. Siegert, M. R. Eshelman, J. A. Kritzer, *Nat. Chem. Biol.* **2014**, *10*, 716-722.

[8] J. M. Berg, J. L. Tymoczko, L. Stryer, *Biochemistry*, 8th ed., W. H. Freeman, New York, **2015**.
[9] V. Nanda, R. L. Koder, *Nat. Chem.* **2010**, *2*, 15-24.
[10] T. Moriuchi, T. Hirao, *Acc. Chem. Res.* **2010**, *43*, 1040-1051.
[11] C. Wang, W. Lai, F. Yu, T. Zhang, L. Lu, X. Jiang, Z. Zhang, X. Xu, Y. Bai, S. Jiang, K. Liu, *Chem. Sci.* **2015**, *6*, 6505-6509.
[12] C. S. Mocny, V. L. Pecoraro, *Acc. Chem. Res.* **2015**, *48*, 2388-2396.
[13] Q. Luo, C. Hou, Y. Bai, R. Wang, J. Liu, *Chem. Rev.* **2016**, *116*, 13571-13632.
[14] T. Machida, S. Dutt, N. Winssinger, *Angew. Chem. Int. Ed.* **2016**, *55*, 8595-8598.
[15] Y. Zhang, M. Herling, D. M. Chenoweth, *J. Am. Chem. Soc.* **2016**, *138*, 9751-9754.
[16] Y. Shi, P. Teng, P. Sang, F. Y. She, L. L. Wei, J. F. Cai, *Acc. Chem. Res.* **2016**, *49*, 428-441.
[17] P. S. Huang, S. E. Boyken, D. Baker, *Nature* **2016**, *537*, 320-327.
[18] F. A. Aldaye, A. L. Palmer, H. F. Sleiman, *Science* **2008**, *321*, 1795-1799.
[19] S. Y. Park, A. K. R. Lytton-Jean, B. Lee, S. Weigand, G. C. Schatz, C. A. Mirkin, *Nature* **2008**, *451*, 553-556.
[20] S. Rinker, Y. G. Ke, Y. Liu, R. Chhabra, H. Yan, *Nat. Nanotechnol.* **2008**, *3*, 418-422.
[21] J. Sharma, Y. G. Ke, C. X. Lin, R. Chhabra, Q. B. Wang, J. Nangreave, Y. Liu, H. Yan, *Angew. Chem. Int. Ed.* **2008**, *47*, 5157-5159.
[22] P. S. Ghosh, A. D. Hamilton, *J. Am. Chem. Soc.* **2012**, *134*, 13208-13211.
[23] M. Humenik, T. Scheibel, *ACS Nano* **2014**, *8*, 1342-1349.
[24] S. I. Liang, J. M. McFarland, D. Rabuka, Z. J. Gartner, *J. Am. Chem. Soc.* **2014**, *136*, 10850-10853.
[25] M. R. Jones, N. C. Seeman, C. A. Mirkin, *Science* **2015**, *347*, 1260901.
[26] H. Eberhard, F. Diezmann, O. Seitz, *Angew. Chem. Int. Ed.* **2011**, *50*, 4146-4150.
[27] E. A. Englund, D. Y. Wang, H. Fujigaki, H. Sakai, C. M. Micklitsch, R. Ghirlando, G. Martin-Manso, M. L. Pendrak, D. D. Roberts, S. R. Durell, D. H. Appella, *Nat. Commun.* **2012**, *3*, 614.
[28] B. M. G. Janssen, E. H. M. Lempens, L. L. C. Olijve, I. K. Voets, J. L. J. van Dongen, T. F. A. de Greef, M. Merkx, *Chem. Sci.* **2013**, *4*, 1442-1450.
[29] S. A. Kazane, J. Y. Axup, C. H. Kim, M. Ciobanu, E. D. Wold, S. Barluenga, B. A. Hutchins, P. G. Schultz, N. Winssinger, V. V. Smider, *J. Am. Chem. Soc.* **2013**, *135*, 340-346.
[30] H. Y. Li, S. H. Park, J. H. Reif, T. H. LaBean, H. Yan, *J. Am. Chem. Soc.* **2004**, *126*, 418-419.
[31] S. H. Park, P. Yin, Y. Liu, J. H. Reif, T. H. LaBean, H. Yan, *Nano Lett.* **2005**, *5*, 729-733.
[32] N. Stephanopoulos, R. Freeman, H. A. North, S. Sur, S. J. Jeong, F. Tantakitti, J. A. Kessler, S. I. Stupp, *Nano Lett.* **2015**, *15*, 603-609.
[33] B. A. R. Williams, C. W. Diehnelt, P. Belcher, M. Greving, N. W. Woodbury, S. A. Johnston, J. C. Chaput, *J. Am. Chem. Soc.* **2009**, *131*, 17233-17241.
[34] O. I. Wilner, Y. Weizmann, R. Gill, O. Lioubashevski, R. Freeman, I. Willner, *Nat. Nanotechnol.* **2009**, *4*, 249-254.
[35] C. Lou, M. C. Martos-Maldonado, C. S. Madsen, R. P. Thomsen, S. R. Midtgaard, N. J. Christensen, J. Kjems, P. W. Thulstrup, J. Wengel, K. J. Jensen, *Nat. Commun.* **2016**, *7*, 12294.
[36] J. Walshaw, D. N. Woolfson, *J. Mol. Biol.* **2001**, *307*, 1427-1450.
[37] A. L. Boyle, D. N. Woolfson, *Chem. Soc. Rev.* **2011**, *40*, 4295-4306.
[38] N. L. Ogihara, M. S. Weiss, W. F. Degrado, D. Eisenberg, *Protein Sci.* **1997**, *6*, 80-88.
[39] L. Malik, J. Nygaard, N. J. Christensen, W. W. Streicher, P. W. Thulstrup, L. Arleth, K. J. Jensen, *J. Pept. Sci.* **2013**, *19*, 283-292.
[40] M. D. Frankkamenetskii, S. M. Mirkin, *Annu. Rev. Biochem.*. **1995**, *64*, 65-95.
[41] K. R. Fox, T. Brown, *Biochem. Soc. Trans.* **2011**, *39*, 629-634.
[42] T. J. Povsic, P. B. Dervan, *J. Am. Chem. Soc.* **1989**, *111*, 3059-3061.
[43] T. Hojland, S. Kumar, B. R. Babu, T. Umemoto, N. Albaek, P. K. Sharma, P. Nielsen, J. Wengel, *Org. Biomol. Chem.* **2007**, *5*, 2375-2379.
[44] J. C. Jewett, C. R. Bertozzi, *Chem. Soc. Rev.* **2010**, *39*, 1272-1279.
[45] J. Dommerholt, S. Schmidt, R. Temming, L. J. A. Hendriks, F. P. J. T. Rutjes, J. C. M. van Hest, D. J. Lefeber, P. Friedl, F. L. van Delft, *Angew. Chem. Int. Ed.* **2010**, *49*, 9422-9425.
[46] G. E. Plum, D. S. Pilch, S. F. Singleton, K. J. Breslauer, *Annu. Rev. Biophys. Biomolec. Struct.* **1995**, *24*, 319-350.
[47] M. Duca, P. Vekhoff, K. Oussedik, L. Halby, P. B. Arimondo, *Nucleic Acids Res.* **2008**, *36*, 5123-5138.
[48] P. Wallimann, R. J. Kennedy, D. S. Kemp, *Angew. Chem. Int. Ed.* **1999**, *38*, 1290-1292.
[49] L. Malik, J. Nygaard, N. J. Cristensen, C. S. Madsen, H. I. Rosner, B. B. Kragelund, R. Hoiberg-Nielsen, W. W. Streicher, L. Arleth, P. W. Thulstrup, K. J. Jensen, *ChemBioChem* **2015**, *16*, 1905-1918.
[50] S. Y. M. Lau, A. K. Taneja, R. S. Hodges, *J. Biol. Chem.* **1984**, *259*, 13253-13261.
[51] N. E. Zhou, C. M. Kay, R. S. Hodges, *J. Biol. Chem*. **1992**, *267*, 2664-2670.
[52] Dassault Systèmes BIOVIA, Discovery studio modeling environment, Release 2017, San Diego: Dassault Systèmes, **2016**.
[53] MacroModel, Schrödinger, LLC, New York, NY, **2016**.
[54] W. L. Jorgensen, J. Chandrasekhar, J. D. Madura, R. W. Impey, M. L. Klein, *J. Chem. Phys.* **1983**, *79*, 926-935.
[55] K. J. Bowers, E. Chow, H. Xu, R. O. Dror, M. P. Eastwood, B. A. Gregersen, J. L. Klepeis, I. Kolossvary, M. A. Moraes, F. D. Sacerdoti, J. K. Salmon, Y. Shan, D. E. Shaw, in *Proceedings of the 2006 ACM/IEEE conference on Supercomputing*, ACM, Tampa, Florida, **2006**, p. 84.
[56] J. L. Banks, H. S. Beard, Y. X. Cao, A. E. Cho, W. Damm, R. Farid, A. K. Felts, T. A. Halgren, D. T. Mainz, J. R. Maple, R. Murphy, D. M. Philipp, M. P. Repasky, L. Y. Zhang, B. J. Berne, R. A. Friesner, E. Gallicchio, R. M. Levy, *J. Comput. Chem.* **2005**, *26*, 1752-1780.
[57] W. Humphrey, A. Dalke, K. Schulten, *J. Mol. Graph.* **1996**, *14*, 33-38.
[58] D. Schneidman-Duhovny, M. Hammel, J. A. Tainer, A. Sali, *Biophys. J.* **2013**, *105*, 962-974.
[59] D. Schneidman-Duhovny, M. Hammel, J. A. Tainer, A. Sali, *Nucleic Acids Res.* **2016**, *44*, W424-W429.

10.1002/chem.201700971

WILEY-VCH

Entry for the Table of Contents (Please choose one layout)

FULL PAPER

A miniature trimeric coiled coil motif was assembled by hybridization of an oligonucleotide triple helix template.

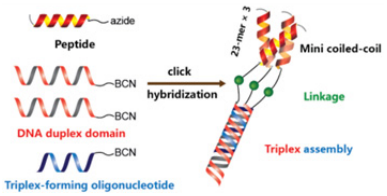

Key Topic* Peptide-oligonucleotide conjugates

Chenguang Lou, Niels Johan Christensen, Manuel C. Martos-Maldonado, Søren Roi Midtgaard, Maria Ejlersen, Peter W. Thulstrup, Kasper K. Sørensen, Knud J. Jensen, and Jesper Wengel**

Page No. – Page No.

Folding Topology of a Short Coiled Coil Peptide Structure Templated by an Oligonucleotide Triplex

*one or two words that highlight the emphasis of the paper or the field of the study